

## Vortex-pair state in rotating superfluid $^3\text{He-A}$ at low temperatures

Kazumi Maki and Xenophon Zotos

*Department of Physics, University of Southern California, Los Angeles, California 90089-0484*

(Received 24 May 1984)

An earlier analysis of the vortex-pair state is extended to lower temperatures. It is shown that the circular-hyperbolic pair describes both the observed transverse satellite frequency and intensity quite well. However, it appears rather difficult to distinguish the radial-hyperbolic pair from the circular-hyperbolic pair. We also predict that the distance between vortices in a pair increases rapidly as the temperature decreases, which can be tested by ultrasonic attenuation.

### I. INTRODUCTION

It is now well established<sup>1</sup> that the vortex-pair state of the type first proposed by Seppälä and Volovik<sup>2</sup> is the only viable candidate for the observed vortex state<sup>3</sup> in rotating superfluid  $^3\text{He-A}$ . Not only the vortex-pair state has much lower free energy<sup>1,2</sup> than the lattice formed by isolated analytic vortices first proposed by Fujita *et al.*<sup>4</sup> but also the observed transverse satellite frequency is inconsistent with that expected from isolated vortices.<sup>1</sup> However, a puzzle remained in our analysis;<sup>1</sup> the vortex-pair state with uniform  $\hat{d}$ , which has obviously higher free energy than that with nonuniform  $\hat{d}$ , appeared to describe better the observed transverse satellite frequency.

The object of this work is to extend the earlier analysis to lower temperatures. For this purpose we shall make use of the texture free energy obtained by Cross<sup>5</sup> (we shall refer to it as Cross's free energy, hereafter). The coefficients in Cross's free energy are evaluated within the weak-coupling theory and with Landau's Fermi liquid coefficients as obtained by Greywall.<sup>6</sup> Although the weak-coupling theory is inadequate to describe the  $A$  phase characterized by the Anderson-Brinkman-Morel condensate, the strong-coupling theory which attempts to describe the  $A$  phase is still at a very primitive stage. Furthermore, we do not believe that the coefficients in Cross's free energy can be off more than 10% when these

coefficients are determined within the weak-coupling theory. Therefore we adopt here the simplest strategy as stated and we believe that our predictions are quantitatively reliable (say, within 10% error).

To our surprise the introduction of the temperature-dependent coefficients clarifies the puzzle which we believe now originated from our unjustified linear extrapolation of the experimental results below  $T=0.85T_c$  to  $T_c$ . In the temperature region where the experimental results are available, the calculated transverse satellite frequency and intensity associated with the circular-hyperbolic pair with nonuniform  $\hat{d}$  agrees well with the observed results (see Fig. 3). Furthermore, we see that the predicted satellite frequency for the vortex pair with uniform  $\hat{d}$  is inconsistent with experiment. On the other hand, our calculation indicates that it is difficult to distinguish the circular-hyperbolic (CH) pair from the radial-hyperbolic (RH) pair by NMR experiment alone. Therefore, our identification of the observed vortex state with the CH pair relies rather on the fact that the free energy of the CH pair is lower than that of the RH pair at all temperatures except possibly at extremely low temperatures (say,  $T < 0.05T_c$ ). We find also that the distance between the two vortices in a vortex pair increases rapidly as the temperature is decreased. This increase in the distance should be readily observable by the ultrasonic attenuation experiment.

### II. FREE ENERGY

Following Cross we shall start with the free energy given by<sup>7</sup>

$$f = \frac{1}{2}\chi_N C_1^2 \int d^3r \{ k_1(\hat{l} \cdot \vec{\nabla} \Phi)^2 + k_2(\hat{l} \times \vec{\nabla} \Phi)^2 + k_3(\vec{\nabla} \Phi)[\text{curl} \hat{l} - \hat{l}(\hat{l} \cdot \text{curl} \hat{l})] - k_4(\vec{\nabla} \Phi) \cdot \hat{l}(\hat{l} \cdot \text{curl} \hat{l}) + k_5(\text{div} \hat{l})^2 + k_6(\hat{l} \times \text{curl} \hat{l})^2 + k_7(\hat{l} \cdot \text{curl} \hat{l})^2 + |(\hat{l} \times \vec{\nabla}) \hat{d}|^2 + \lambda |(\hat{l} \cdot \vec{\nabla}) \hat{d}|^2 + \xi_1^{-2}[1 - (\hat{l} \cdot \hat{d})^2] + \xi_H^{-2} \hat{d}_z^2 \} , \tag{1}$$

where the  $k_i$  coefficients given in the Appendix are temperature dependent and are expressed in terms of the number  $\rho_{s\perp}$ ,  $\rho_{s\parallel}$ , and spin  $\rho_{s\perp}^{\text{sp}}$ ,  $\rho_{s\parallel}^{\text{sp}}$  superfluid densities.  $\xi_1 = C_1(T)/\Omega_A(T)$  is the dipole-coherence length and

$$\xi_H = (\Delta\chi/\chi_N)^{-1/2} C_1(T)/(\gamma H) = (H_0/H)\xi_1$$

is the magnetic coherence length. Here,  $\Delta\chi$  is the anisotropic part of the spin susceptibility. The dipole-coherence length  $\xi_1$  defined here<sup>7</sup> differs somewhat from the conventional one, as we introduce the length scale through  $C_1$  the spin-wave velocity in the transverse direction to the  $\hat{l}$  vector. However, we find that the present

definition is not only convenient for the analysis of the nuclear magnetic resonance satellite frequency but also that  $\xi_{\perp}$  thus defined is almost temperature independent; within the whole temperature range  $(0, T_c)$  it changes only less than a few percent. Therefore we shall take  $\xi_{\perp}$  ( $\approx 10 \mu\text{m}$ ) a constant independent of  $T$ . The free energies of the vortex-pair states will be determined variationally. We shall consider in the following the circular-hyperbolic pair and the radial-hyperbolic pair separately. For the CH vortex pair we choose as a variational solution<sup>1</sup>

$$\alpha = \phi_1 + \phi_2, \quad \gamma = -\phi_1 + \phi_2 + \frac{\pi}{2},$$

$$\cos\beta = \cos v [f(u)], \quad \chi = \pi/2,$$

$$\sin\psi = 1 - 2 \sin^2 v (\sin^2 v + \theta^2)^{-1},$$

where

$$\phi_1 = \tan^{-1} \left[ \frac{y}{x-c} \right], \quad \phi_2 = \tan^{-1} \left[ \frac{y}{x+c} \right], \quad (2)$$

$$\theta = \sinh u + \frac{(\sinh b)^2}{\sinh u}, \quad f(u) = e^{-a(\cosh u - 1)},$$

and  $u, v$  are defined by

$$x = c \cosh u \cos v, \quad (3)$$

$$y = c \sinh u \sin v.$$

In Eq. (1)  $\hat{l}$ ,  $\hat{d}$ , and  $\vec{\nabla}\Phi$  are expressed in terms of the Euler angles  $\alpha, \beta, \gamma, \chi, \psi$  as follows:

$$\begin{aligned} \vec{\nabla}\Phi &= \vec{\nabla}\alpha + \cos\beta \vec{\nabla}\gamma, \\ \hat{l} &= (-\sin\beta \cos\gamma)\hat{x} + (\sin\beta \sin\gamma)\hat{y} + \cos\beta\hat{z}, \\ \hat{d} &= (-\cos\psi \sin\chi)\hat{x} + (\sin\psi \sin\chi)\hat{y} + \cos\chi\hat{z}. \end{aligned} \quad (4)$$

In Eqs. (2) and (3) the variational parameters are  $a, b$ , and  $c$ ;  $a$  describes how fast the  $\hat{l}$  vector approaches the horizontal plane from the vertical direction at the center of the  $2\pi$  vortices,  $b$  describes the deviation from the uniform  $\hat{d}$  texture, and  $2c$  is the distance between vortices in the pair.

As in Ref. 1 we cut off the integral at  $r = r_0$ , the distance between two vortex pairs. The free energy is minimized at different temperatures. For  $F_1^s$  and  $F_1^a$  we have used  $F_1^s = 13.2$  and  $F_1^a = -0.98$  values appropriate for liquid  $^3\text{He}$  at  $P = 29$  bar taken from Greywall<sup>6</sup> (although we find that the results are practically identical for 21 bar and melting pressure). The free energy for the vortex pair per unit length is given by

$$\begin{aligned} f &= 2\pi \left[ \frac{\hbar}{2m_3} \right]^2 (\rho_{s\parallel} + \rho_{s\perp}) \ln(r_0/\xi_{\perp}) \\ &+ \frac{\pi}{4} \left[ \frac{\hbar}{2m_3} \right]^2 \rho_{s\perp}^{\text{spin}} \Delta f, \end{aligned} \quad (5)$$

where the first term describes the free energy due to the

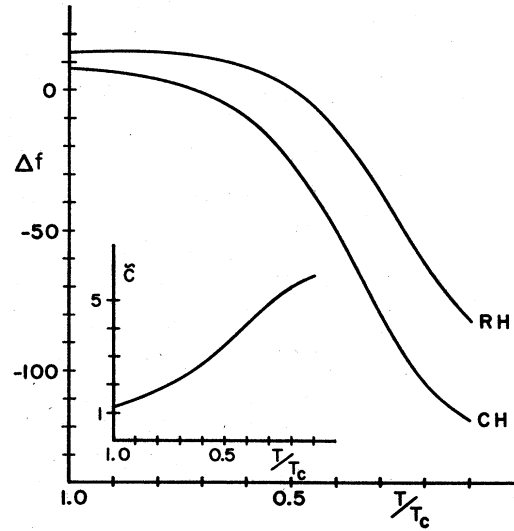


FIG. 1. Free energy  $\Delta f$  and intervortex distance in a pair  $c$  as a function of reduced temperature  $T/T_c$  for a circular-hyperbolic and radial-hyperbolic pair.  $\bar{c}$  is practically coincident for the CH and RH pair.

circulation of  $4\pi$ . Here,  $r_0$  is the intervortex pair distance  $(\pi n_v)^{-1/2}$  and Eq. (5) is valid for  $r_0 > 10\xi_{\perp}$ .  $\Delta f$  in Eq. (5) is shown in Fig. 1 along with the pair distance  $c$ .  $\Delta f$  decreases monotonically as the temperature decreases. We have repeated a similar calculation for the RH pair where the expression for  $\gamma$  and  $\sin\psi$  are replaced by

$$\gamma = -\phi_1 + \phi_2, \quad \cos\psi = 1 - 2 \sin^2 v (\sin^2 v + \theta^2)^{-1}. \quad (6)$$

The results of the minimization are shown again in Fig. 1. We note that in all the temperature region we have studied ( $T \geq 0.1T_c$ ), the CH pair is more stable than the RH pair although the difference in the free energies is not so

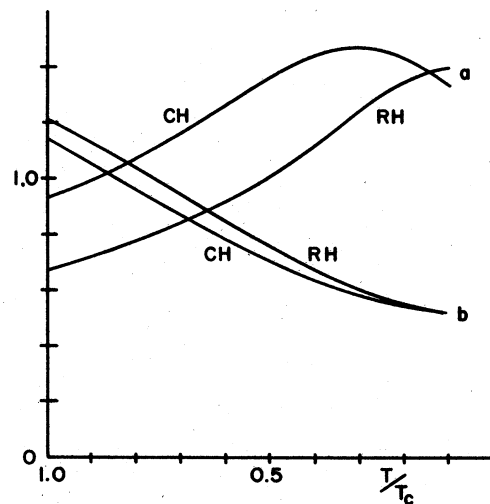


FIG. 2. Variational coefficients  $a$  and  $b$  as function of reduced temperature  $T/T_c$ .

large. We show the corresponding variation parameters  $a$  and  $b$  as functions of  $t = T/T_c$  the reduced temperature in Fig. 2. In the vicinity of  $T_c$ ,  $a$  and  $c$  increase initially while  $b$  decreases which is due to the fact that  $\rho_{s\parallel}, \rho_{s\perp}$ , etc., related to the mass superflow, increase much faster than  $\rho_{s\parallel}^{\text{spin}}$ , etc. related to the spin flow. In particular, the monotonic increase of  $\tilde{c} = c/\xi_{\perp}$  with decreasing temperature is due to the fact that  $\rho_{s\parallel}/\rho_{s\parallel}^{\text{spin}}$  increases also monotonically for example; the reduction of the elastic energy associated with the spatial derivatives of  $\alpha$  and  $\gamma$  are achieved by increasing  $c$ . Since  $c$  changes by a factor of 5

or 6 as temperature changes from  $T_c$  to  $0.1T_c$ , this large temperature dependence should be readily accessible by ultrasonic attenuation (see Sec. IV). Finally,  $a$  shows a small curious peak around  $T = 0.35T_c$  for the CH pair, while no such peak appeared for the RH pair. This small peak is due to the fact that  $k_6$  (which controls the bending energy) still keeps increasing around  $T \approx 0.3T_c$ , while most other coefficients have saturated in this temperature region. Therefore for the RH pair whose vortex free energy is mostly controlled by  $k_5$  (the splay energy),  $a$  continues to increase monotonically.

### III. MAGNETIC RESONANCES

The nuclear magnetic resonance satellite frequencies are determined by solving the eigenvalue equations.<sup>1,8</sup> These equations are cast in the variational form which is more convenient for our purpose:

$$\begin{aligned} \lambda_t = \int \int dx dy & \{ \cos^2\beta |\vec{\nabla} g_1|^2 + \sin^2\beta [\sin(\gamma)g_{1x} + \cos(\gamma)g_{1y}]^2 - \{ \cos^2\beta |\vec{\nabla}\psi|^2 + [\sin(\gamma)\psi_x + \cos(\gamma)\psi_y]^2 \} g_1^2 \\ & + \lambda \{ \sin^2\beta [\cos(\gamma)g_{1x} - \sin(\gamma)g_{1y}]^2 - \sin^2\beta [\cos(\gamma)\psi_x - \sin(\gamma)\psi_y]^2 g_1^2 \} \\ & + \xi_{\perp}^{-2} [\sin^2\beta \cos^2(\gamma - \psi) - \cos^2\beta] g_1^2 \} / \langle g_1^2 \rangle, \end{aligned} \quad (7)$$

$$\begin{aligned} \lambda_l = \int \int dx dy & \{ \cos^2\beta |\vec{\nabla} g_2|^2 + \sin^2\beta [\sin(\gamma)g_{2x} + \cos(\gamma)g_{2y}]^2 \\ & + \lambda \sin^2\beta [\cos(\gamma)g_{2x} - \sin(\gamma)g_{2y}]^2 + \xi_{\perp}^{-2} \sin^2\beta [2 \cos^2(\gamma - \psi) - 1] g_2^2 \} / \langle g_2^2 \rangle, \end{aligned} \quad (8)$$

where  $g_1$  and  $g_2$  are the variational wave functions describing the transverse and longitudinal spin oscillations, respectively.

The transverse and longitudinal satellite frequencies are given in terms of  $\lambda_t$  and  $\lambda_l$  as

$$\omega_t^{\text{sat}} = [(\gamma H)^2 + \lambda_t \Omega_A^2]^{1/2} \cong \gamma H + \frac{\lambda_t}{2} \Omega_A (\gamma H)^{-1}, \quad (9)$$

$$\omega_l^{\text{sat}} = (\lambda_l)^{1/2} \Omega_A. \quad (10)$$

Furthermore, the intensity of the satellite for a single vortex pair of unit length is given by

$$I_t = \left[ \left| \int dx dy g_1 \cos\psi \right|^2 + \left| \int dx dy g_1 \sin\psi \right|^2 \right] / \int dx dy |g_1|^2, \quad (11)$$

$$I_l = \left| \int dx dy g_2 \right|^2 / \int dx dy |g_2|^2, \quad (12)$$

respectively. We have determined  $\lambda_t$  and  $\lambda_l$  variationally by using a couple of different variational functions. We find near  $T = T_c$  where the binding energy of the bound spin-wave state is small that

$$g_{1,2} \propto e^{-\mu(chu-1)} \quad (13)$$

is an excellent variation function. While in the case of the transverse resonance, we find

$$g_1 \propto e^{-(\mu/2)(chu - \cos\psi)^2} + e^{-(\mu/2)(chu + \cos\psi)^2} \quad (14)$$

gives a lower  $\lambda_t$  value at low temperatures. The results for the transverse and longitudinal satellites are summarized in Figs. 3 and 4. In Fig. 3 we show  $\lambda_t$  for both the CH and RH pair as a function of  $t$ . In the inset, the nor-

malized satellite intensity  $\tilde{I}_t = n_v I_t / \Omega I_0 = 0.0015 I_t / I_0$  with  $n_v$  the vortex-pair density and  $\Omega$  the rotation speed is shown as a function of  $t$ . The shaded area is constructed from the experimental data by Hakonen *et al.*<sup>3</sup> We see immediately that the CH pair describes quite well both

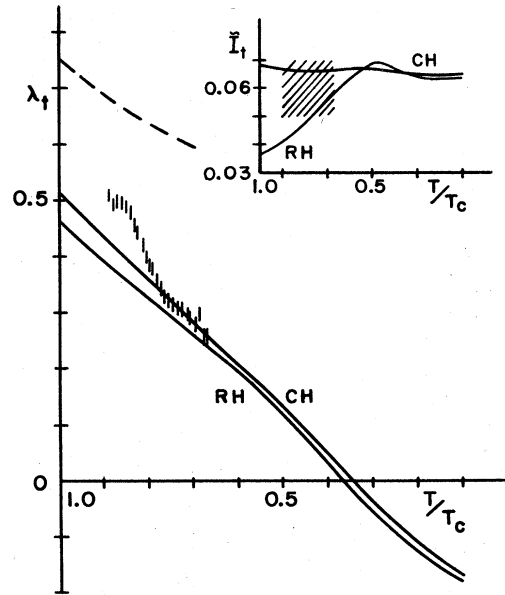


FIG. 3. Eigenvalues  $\lambda_t$  of transverse spin oscillations as a function of  $T/T_c$ ; full lines for circular-hyperbolic and radial-hyperbolic pair with nonuniform  $\hat{a}$ ; in the insert the corresponding intensities. The broken line represents the CH pair with uniform  $\hat{a}$ ; shaded area represents the experimental results.

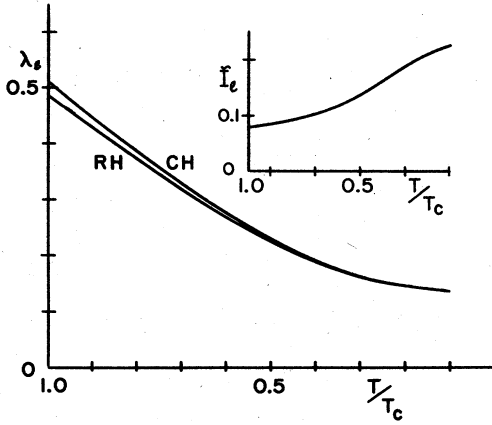


FIG. 4. Eigenvalues  $\lambda_l$  of longitudinal spin oscillations as a function of  $T/T_c$  for a CH and RH pair with nonuniform  $\hat{d}$ ; the inset represents the corresponding intensities.

the observed transverse satellite frequency and intensity. In particular, below  $T=0.8T_c$  the agreement between the theory and the experiment is excellent. It becomes clear that the satellite frequency associated with the CH pair with uniform  $\hat{d}$  as indicated by a dotted line is far off the experimental value. Therefore the puzzle was nothing but an artifact of wrong extrapolation of the experimental data to  $T=T_c$ . On the other hand, we also see that the RH pair describes almost as well the observed satellite frequency and the satellite intensity. In particular, at low temperatures, these two vortex pairs produce a satellite frequency and intensity almost identical to each other. Therefore the NMR experiment is not suitable to discriminate these two vortex-pair configurations.

We note that  $\lambda_t$  decreases almost linearly with  $t$  and crosses  $\lambda_t=0$  around  $t=0.35$ . This implies that in a weak magnetic field ( $H \simeq H_0$ ), the  $\hat{d}$  configuration becomes unstable in buckling in the plane perpendicular to the  $x$ - $y$  plane below  $T < 0.35T_c$ . In other words, the vortex-pair texture changes gradually as the external magnetic field is lowered even when  $H$  is still larger than  $H_0$ .

#### IV. SOUND ATTENUATION

Since ultrasonic attenuation depends sensitively on the relative orientation of  $\hat{l}$  to the propagation direction of the sound wave, it provides another useful probe for the study of the underlying  $\hat{l}$  texture.<sup>9</sup> When  $\hat{l}$  makes an angle  $\theta$  from  $\vec{q}$ , the propagation vector of the longitudinal sound wave, the attenuation coefficient is given by<sup>10,11</sup>

$$\alpha(\theta) = \alpha_0 + \alpha_{||} \cos^4 \theta + \alpha_{\perp} \sin^4 \theta + 2\alpha_c \sin^2 \theta \cos^2 \theta, \quad (15)$$

where  $\alpha_0$  is the  $\theta$  independent part and  $\alpha_0$ ,  $\alpha_{||}$ ,  $\alpha_{\perp}$ , and  $\alpha_c$  depend on both temperature and sound frequency. For example  $\alpha_{\perp}$  has a sharp peak associated with the clapping mode, while  $\alpha_c$  has a broad peak due to the normal flapping mode.<sup>11</sup> In the absence of vortices  $\hat{l}$  is assumed to be uniform and lie in the  $\hat{y}$  direction. This situation is prepared by tilting the external magnetic field from the

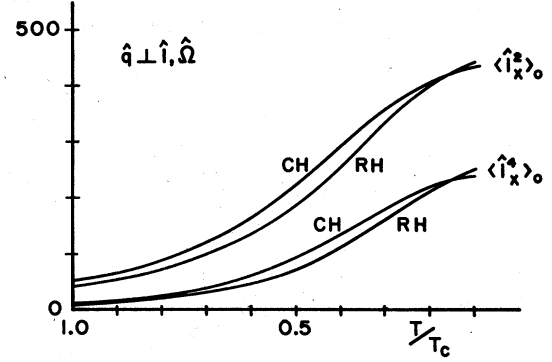


FIG. 5.  $\langle \hat{l}_x^2 \rangle_0$ ,  $\langle \hat{l}_x^4 \rangle_0$  as a function of reduced temperature  $T/T_c$  for  $\vec{q} \perp \hat{l}, \hat{\Omega}$ .

rotation axis (in the  $z$  direction) slightly towards the  $\hat{x}$  direction. In the presence of vortex pairs then the  $\hat{l}$  configuration is disturbed; the vortex pairs orient  $\hat{l}$  in their vicinity both in the  $\hat{x}$  and the  $\hat{z}$  direction. Then when the sound wave propagates along the  $\hat{x}$  direction for example, the attenuation coefficient within the local approximation<sup>9</sup> is given by

$$\alpha_x = \alpha_0 + \alpha_{||} \langle \hat{l}_x^4 \rangle + \alpha_{\perp} \langle (1 - \hat{l}_x^2)^2 \rangle + 2\alpha_c \langle (1 - \hat{l}_x^2) \hat{l}_x^2 \rangle, \quad (16)$$

where  $\langle \hat{l}_x^4 \rangle$  is the space average of  $\hat{l}_x^4$  with  $\hat{l}_x$  representing the  $x$  component of  $\hat{l}$ . Since the deviation of the  $\hat{l}$  vector from the uniform  $\hat{y}$  direction is proportional to the vortex-pair density, we can express  $\langle \hat{l}_x^4 \rangle$  and  $\langle \hat{l}_x^2 \rangle$  by

$$\langle \hat{l}_x^4 \rangle = n_v \xi_1^2 \langle \hat{l}_x^4 \rangle_0$$

and

$$\langle \hat{l}_x^2 \rangle = n_v \xi_1^2 \langle \hat{l}_x^2 \rangle_0, \quad (17)$$

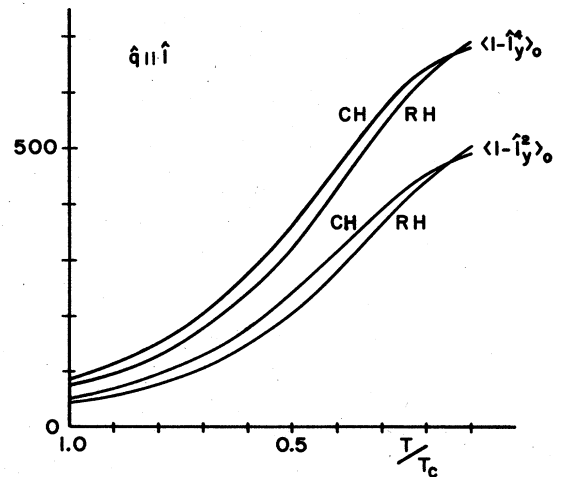


FIG. 6.  $\langle 1 - \hat{l}_y^2 \rangle_0$ ,  $\langle 1 - \hat{l}_y^4 \rangle_0$  as a function of reduced temperature  $T/T_c$  for  $\vec{q} \parallel \hat{l}$ .

where the subscript 0 means that the integral is made for a single vortex pair, for example,

$$\langle \hat{l}_x^2 \rangle_0 = \int du \int dv c^2 (ch^2 u - \cos^2 v) \cos^2 \gamma \sin^2 \beta. \quad (18)$$

Then Eq. (16) is rewritten as

$$\alpha_x = \alpha_0 + \alpha_1 + n_v \xi_1^2 [(\alpha_{||} + \alpha_1 - 2\alpha_c) \langle \hat{l}_x^4 \rangle_0 - 2(\alpha_1 - \alpha_c) \langle \hat{l}_x^2 \rangle_0]. \quad (19)$$

The coefficients  $\langle \hat{l}_x^2 \rangle_0$  and  $\langle \hat{l}_x^4 \rangle_0$  are evaluated numerically and shown as a function of reduced temperature in Fig. 5 for both the CH and RH pair for  $r_0 = 20\xi_1$ . Similarly, the attenuation coefficients for  $\vec{q}$  parallel to the rotation axis ( $\hat{z}$  axis) and  $\vec{q}$  parallel to the  $\hat{y}$  axis (parallel to the asymptotic  $\hat{l}$  direction) are expressed in terms of  $\langle \hat{l}_z^2 \rangle_0$ ,  $\langle \hat{l}_z^4 \rangle_0$  and  $\langle 1 - \hat{l}_y^2 \rangle_0$ ,  $\langle 1 - \hat{l}_y^4 \rangle_0$ , respectively. In the last two coefficients we subtracted 1 in order to eliminate the contribution associated with the uniform  $\hat{l}$  texture and thus obtain the local vortex contribution. These are plotted in Figs. 6 and 7 as functions of reduced temperature. We note that both  $\langle \hat{l}_x^2 \rangle_0$ ,  $\langle \hat{l}_x^4 \rangle_0$  and  $\langle 1 - \hat{l}_y^2 \rangle_0$ ,  $\langle 1 - \hat{l}_y^4 \rangle_0$  increase rapidly as the temperature decreases, while the temperature dependence of  $\langle \hat{l}_z^2 \rangle_0$ ,  $\langle \hat{l}_z^4 \rangle_0$  is rather moderate. In particular, at low temperatures  $\langle \hat{l}_z^2 \rangle_0$  and  $\langle \hat{l}_z^4 \rangle_0$  are roughly by a factor of  $10^{-1}$  smaller than  $\langle \hat{l}_x^2 \rangle_0$  and  $\langle \hat{l}_x^4 \rangle_0$ . These behaviors reflect the fact that the  $\langle \hat{l}_x^2 \rangle_0$  and  $\langle \hat{l}_y^2 \rangle_0$  coefficients increase with  $c$ , the distance between the vortices in a pair, while  $\langle \hat{l}_z^2 \rangle_0$  is a measure only of the size of individual vortices and thus proportional to  $a^{-1}$ . Therefore we conclude that the most favorable configuration to send the sound wave is the  $\hat{x}$  direction perpendicular to the asymptotic  $\hat{l}$  direction. Although the temperature dependences of these coefficients for the CH and the RH pair are rather similar, the RH pair gives rise to the attenuation coefficient 10 to 20% smaller than that of the CH pair. Therefore the sound attenuation technique could be used to discriminate these two different configurations.

#### APPENDIX

The  $k_i$  coefficients in the Cross free-energy expression are given by<sup>7</sup>

$$k_1 = \rho_{s||} / \rho_{s\perp}^{\text{spin}}, \quad k_2 = \rho_{s\perp} / \rho_{s\perp}^{\text{spin}}, \quad k_3 = k_2 (\rho_{s||}^0 / \rho_{s\perp}^0), \quad k_4 = k_1, \quad k_5 = \frac{1}{4} (1 + \frac{1}{3} F_1^s)^{-1} \rho_{s\perp}^0 / \rho_{s\perp}^{\text{spin}},$$

$$k_6 = \frac{1}{3} (1 + \frac{1}{3} F_1^s)^{-1} \left[ \frac{1}{4} \rho_{s\perp}^0 + \rho_{s||}^0 + \frac{1}{4} \frac{F_1^s}{1 + \frac{1}{3} F_1^s (\rho_{n||}^0 / \rho)} \rho_{s||}^0 (\rho_{s||}^0 / \rho) \right] / \rho_{s\perp}^{\text{spin}},$$

$$\lambda = \rho_{s||}^{\text{spin}} / \rho_{s\perp}^{\text{spin}}, \quad \chi_N C_1^2 = (\hbar/2m)^2 \rho_{s\perp}^{\text{spin}},$$

where

$$\rho_{s\perp,||} = \frac{1}{1 + \frac{1}{3} F_1^s (\rho_{n\perp,||} / \rho)} \rho_{s\perp,||}^0$$

is the superfluid mass density including Fermi liquid corrections, and

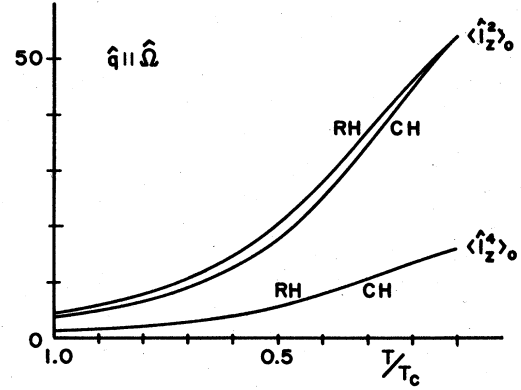


FIG. 7.  $\langle \hat{l}_z^2 \rangle_0$ ,  $\langle \hat{l}_z^4 \rangle_0$  as a function of reduced temperature  $T/T_c$  for  $\vec{q} \parallel \hat{\Omega}$ .

#### V. CONCLUDING REMARKS

We have extended our earlier analysis at low temperatures. We find that (1) the CH pair has always lower free energy than the RH pair. (2) The CH pair produces both the transverse satellite frequency and the satellite intensity consistent with observation. (3) However, since the RH pair described almost as well the NMR experiment, we need another probe (say, ultrasonic attenuation) in order to discriminate these two configurations. (4) We find that  $c$ , the distance between vortices in the pair, increases rapidly as the temperature decreases. (5) We calculate the change in the sound attenuation coefficient in the presence of the vortex pair. We find that this change increases rapidly at lower temperatures in the appropriate geometry, which reflects the temperature dependence of  $c$ .

#### ACKNOWLEDGMENTS

We would like to thank Martti Salomaa for sending us results prior to publication. This work is supported by the National Science Foundation under Grant No. DMR-82-14525.

$$\rho_{s\perp,||}^{\text{spin}} = \frac{1 + \frac{1}{3} F_1^a}{1 + \frac{1}{3} F_1^a (\rho_{n\perp,||} / \rho)} \frac{1}{1 + \frac{1}{3} F_1^s} \rho_{s\perp,||}^0$$

is the superfluid spin density including Fermi liquid correlations. The temperature dependence of the superfluid densities  $\rho_{s\perp}^0, \rho_{s||}^0$  are calculated from the temperature dependence of the gap.<sup>12</sup>

- <sup>1</sup>X. Zotos and K. Maki, Phys. Rev. B 30, 145 (1984).
- <sup>2</sup>H. K. Seppälä and G. E. Volovik, J. Low Temp. Phys. 51, 279 (1983).
- <sup>3</sup>P. J. Hakonen, O. T. Ikkala, S. T. Islander, O. V. Lounasmaa, and G. E. Volovik, J. Low Temp. Phys. 53, 425 (1983); H. K. Seppälä, P. J. Hakonen, M. Krusius, T. Ohmi, M. M. Salomaa, J. T. Simola, and G. E. Volovik, Phys. Rev. Lett. 52, 1802 (1984).
- <sup>4</sup>T. Fujita, M. Nakahara, T. Ohmi, and T. Tsuneto, Prog. Theor. Phys. 60, 671 (1978); see also A. L. Fetter, J. A. Sauls, and D. L. Stein, Phys. Rev. B 28, 5061 (1983).
- <sup>5</sup>M. C. Cross, J. Low Temp. Phys. 21, 525 (1975).
- <sup>6</sup>D. S. Greywall, Phys. Rev. B 27, 2747 (1983).
- <sup>7</sup>K. Maki and P. Kumar, Phys. Rev. B 17, 1088 (1978).
- <sup>8</sup>K. Maki, Phys. Rev. B 27, 4173 (1983).
- <sup>9</sup>M. Nakahara, T. Ohmi, T. Tsuneto, and T. Fujita, Prog. Theor. Phys. 62, 874 (1979).
- <sup>10</sup>D. N. Paulson, M. Krusius, and J. C. Wheatley, J. Low Temp. Phys. 26, 73 (1977).
- <sup>11</sup>For a review see P. Wölfle, in *Progress in Low Temperature Physics*, edited by D. F. Brewer (North-Holland, Amsterdam, 1978), Vol. VIIa.
- <sup>12</sup>R. Combescot, J. Low Temp. Phys. 18, 537 (1975).